Nanotechnology 7 (1996) 447–451. Printed in the UK

Pattern transfer to silicon by microcontact printing and RIE

Thomas K Whidden†, David K Ferry†, Michael N Kozicki†, Enoch Kim‡, Amit Kumar‡, James Wilbur‡ and George M Whitesides‡

† College of Engineering and Applied Science, Center for Solid State Electronics, Arizona State University, Tempe, AZ 85287, USA
‡ Department of Chemistry, Harvard University, 12 Oxford Street, Cambridge, MA 02138, USA

Abstract. Microcontact printing techniques employing self-assembled alkanethiol monolayers in the production of metal masks have been combined with CF_4/O_2 reactive ion etch for subsequent pattern transfer to silicon. Silicon feature sizes of about 300 nm have been demonstrated. Some inadequacies in the self-assembled monolayers (SAMs)-formed metal masks have been characterized by electron microscopy. Particularly, nickel etch control and metal feature edge definition remain problems to be solved if the process is to be employed in submicron feature production. Nickel patterns produced in the process and used as masks without the gold overlayer were successful as masks in the reactive ion etching (RIE) process. They also appear to give a somewhat improved edge definition over processes in which the gold layer remains.

1. Introduction

The continued drive to denser packing in integrated semiconductor devices has resulted in a broad and intensive exploration of various means of pattern generation for device feature generation. Optical techniques, historically the primary methodology in device manufacture [1], have evolved to utilize ever shorter wavelengths in efforts to achieve feature dimensions and enhanced resolution from polymeric photoresists [2]. Optical methods may be reaching the limits of applicability, however, due to problems with resist transparency, standing wave effects and depth of focus [3]. It is near certainty that optical methods will not be adequate for nanoscale lithography (below 100 nm).

Alternative methods in submicron and nanometer-scale lithography include the use of high-energy electron and ion beams as well as x-rays in the definition of features in conventional polymeric resists. Such methods have been successfully employed in creating features with dimensions in the 20–100 nm range [4–6]. Unfortunately, approaches employing conventional polymeric resists have inherent limitations arising from such factors as proximity effects and electron scattering. These deficiencies in conventional resist systems have resulted in a current, very active exploration of ultrathin alternative resist materials in a variety of approaches to lithographic patterning [2, 7–11].

Self-assembled monolayers (SAMs) [12–14] on various substrates have recently shown very encouraging results as ultrathin resists in quasi-conventional lithographic processes for GaAs [7], SiO_2 [7] and various metals [9, 10]. Patterning techniques that have been used with SAMs include micromachining [15], ion- and electron-beam lithographies [16], microwriting [17, 18] and photolithography/oxidative patterning with UV light [19, 20]. Additionally, a unique and extremely simple new methodology for patterning gold films using microcontact printing techniques and SAMs has recently been developed within the Whitesides group at Harvard [22].

We report here on the morphological and elemental composition of metal masks produced using microcontact printing techniques and on the use of the masks thus created in the transfer of patterns to underlying silicon substrates.

2. Experimental

Patterned silicon/nickel/gold structures were prepared as reported in [23]. Substrates were silicon wafers upon which a composite structure consisting of 50 nm of nickel followed by 25 nm of gold had been deposited by electron-beam evaporation. The metal mask patterns were generated using an elastomeric stamp that transfers an alkanethiol 'ink' to a gold surface by contact; if the stamp was patterned, a patterned SAM forms. The stamp was fabricated by casting poly(dimethylsiloxane) (PDMS) on a master having the desired pattern. Masters were prepared using standard photolithographic techniques, or constructed from existing materials having microscale surface features. 'Inking' of the master was accomplished by exposing the stamp to a 0.1–1.0 mM solution of alkanethiol in anhydrous ethanol, either by pouring the solution on the surface of the stamp, or by rubbing the stamp gently with a Q-tip that had been saturated with the inking solution. The

0957-4484/96/040447+05$19.50

stamp was allowed to dry until no liquid was visible to the eye, then applied (typically by hand) to a gold surface. Very light hand pressure was used to aid in complete contact between the stamp and the surface. Following SAM pattern formation, substrates were immersed in a solution of KCN (0.1–1.0 mM) and KOH (1 M) in order to remove the exposed gold. The solution was stirred and oxygen was continuously bubbled through the solution during etching. Nickel (and presumably the residual SAMs) was removed by submerging the substrate in a mixture of H_2SO_4, 30% H_2O_2, H_3PO_4 and 30% $NiSO_4$ (5:5:1:4 by volume respectively).

The stamped features were evaluated as masks in reactive ion etching processes. Etch experiments were performed using a plasmalab reactive ion etcher equipped with BCl_3, Cl_2, CF_4 and O_2 gas feeds. An initial series of experiments evaluating the use of BCl_3/Cl_2 for an etchant process was abandoned due to poor observed etch rates and an apparent gas/metal interaction, as determined from electron micrographs. A series of experiments was performed to test various CF_4/O_2 mixtures, RF powers and pressures as etchant systems. Satisfactory results for preliminary studies were obtained with a CF_4/O_2 mixture of 25 sccm: 10 sccm, RF power of 100 W and an etch process pressure of 100 mTorr. These settings were found to produce a 1 micron deep pattern in silicon with minimal apparent interaction with the metal mask.

Following reactive ion etching (RIE) pattern transfer to the silicon substrate, the metal mask structure was removed prior to silicon pattern characterization. Generally, the metal composite structure was removed in aqua regia. In a certain instance, the gold was removed prior to nickel etching using a commercial gold etchant containing KCN (Union Etchants International Inc., gold etch solution UN 1935). Nickel layers exposed by the removal of the gold were etched using aqua regia.

Metal pattern feature heights and patterned silicon etch depths were determined using a Sloan Dektak profilometer. Electron micrographs of the starting patterns and etched features were obtained using either an ISI DS-130 or JEOL JXA-840 scanning electron microscope (SEM). The JEOL SEM was equipped with a Tracor-Northern Energy Dispersive x-ray analyzer which was used in the determination of elemental compositions and residual metals.

3. Discussion

Figures 1 and 2 present electron micrographs of the metal pattern, as formed using the microcontact printing technique. It may be seen from figure 1 that all of the larger metal features exhibit a brightness/contrast substructure in the micrographs. This structure consists of a brighter area in the central part of each feature surrounded by a perimeter band of reduced brightness. Below a certain critical feature size, the brighter, central feature is not apparent. A more detailed examination of the edge structure of the metal features is shown in figure 2. Each metal feature produced in the microcontact printing process exhibits a substructure of at least two, and often three,

Figure 1. A microcontact pattern in a Au/Ni metal layer defined by a SAM 'stamped' pattern on Si/SiO_2.

components. At the very edge of every feature, a perimeter band possessing a granular film structure is observed, with the bandwidth usually about 500 nm. Occasionally, this granular region is observed to be much wider. A detailed SEM examination of the edge band (not shown) suggests that the average diameter of individual granules is about 30 nm. The granularity may be a result of increased permeability of the SAM near the pattern edge with consequent, but limited etching of the gold by the cyanide solution. Individual grains appear to be columnar and an underlying connectivity between grains is suggested by high resolution SEM, but is not definitive. Inward from the perimeter of each feature, another area of relatively low SEM brightness is observed. The width of this band is variable between samples but appears to be relatively consistent for features on the same sample. The detail in figure 2 shows the area to be a continuous film structure, albeit heavily populated with what appear to be pinholes. Finally, larger metal features show a central area of high SEM brightness, a portion of which is evident in figure 1. It may be seen that, aside from the brightness differences, the inner perimeter band and the central area of the metal features are essentially identical, continuous films, both with a significant number of pinholes.

The feature substructure apparent from the electron micrographs prompted us to examine the elemental composition of the various areas in the metal film. An Auger sputter profile of the central, bright area of a large metal feature was performed. The elemental distribution was consistent with the expected structure of the composite metal layer. Of somewhat more interest are elemental composition comparisons between the different substructures discussed above. Figure 3 shows a metal feature exhibiting all three substructures. EDS line scan elemental analyzes of the feature shows distinct compositional differences between the two perimeter band structures and the central, bright region of the feature. It may be seen that the perimeter bands of lower SEM brightness are composed of only gold, whereas the brighter regions give signals for the expected nickel/gold composite structure. Signal intensities are consistent with the expected structure when EDS penetration depths and interaction

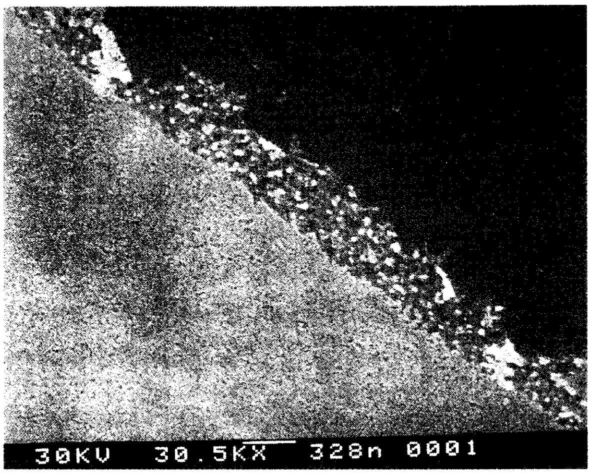

Figure 2. Edge detail (marked 'A' and arrow) showing the granularity of the outer structure of the overlaying Au film.

spheres are considered. Elemental composition data suggest a rationale for the brightness contrasts observed in the electron micrographs. Areas of high SEM brightness in the metal features are thought to arise from enhanced backscatter of the electron beam due to the presence of nickel (atomic number 28) under these regions of the gold versus silicon (atomic number 14) under the areas of lower brightness. The consistent presence of darker areas at the perimeter of features suggests that the loss of nickel is due to an overlong or a too aggressive metal etch. Using the electron micrographs as a diagnostic tool, this problem should be readily minimized. Control of the rate of nickel etch under very narrow features may prove critical to the process, therefore it may be advantageous to examine a more directional etch (RIE?) for future routes to nickel removal in the microcontact printing process.

A potentially more serious problem with the metal mask formation may be the presence of the granular perimeter band apparent in figure 2. Such a structure might be expected to present a relatively porous barrier to etchant gases in the RIE process with consequent problems of edge definition for features produced. The literature suggests that alkanethiol layers consist of well ordered domains with dimensions of about 20–30 nm in diameter. These domains are separated by boundary regions which exhibit a significant degree of disorder. The domain boundaries would be expected to function less effectively as a barrier layer between etch solutions and the underlying gold. The pinhole density in the continuous gold films may reflect this domain boundary effect. It may be that SAMs formed from the edge of the stamp features are inherently less well ordered than those from central areas of a stamp pattern feature. One would expect, then, that the barrier effectiveness near metal feature edges is significantly poorer with consequent generation of the observed granularity. SEM-determined granule size is consistent with the calculated domain size for these SAMs. If this is, indeed, the cause of the granular edge character, it may represent a significant impediment to the use of microcontact printing in submicron structure generation.

Figures 4–6 show electron micrographs of the silicon surface after the masked substrate had been subjected to

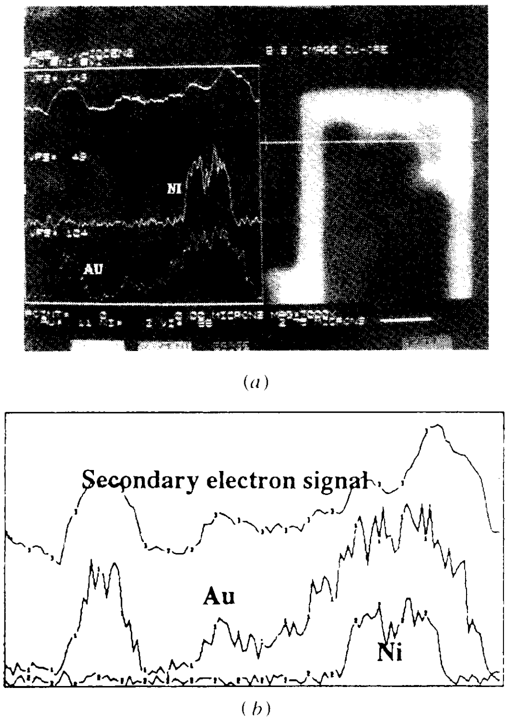

Figure 3. The EDS linescans for the various elements (*a*) are replotted in expanded view (*b*). The image area being scanned is shown in (*a*) as well.

the RIE process and the metal mask removed in aqua regia. A detailed examination of the features in figure 4 suggests that there is a slight, but significant etch rate enhancement evident at the perimeter of each area that had been protected by the metal masking layer. Such a rate enhancement is consistent with the presence of an overhanging gold film structure that formed when the underlying nickel was over-etched. It would be expected that, from simple ballistic considerations, some increase in the probability of etchant/substrate interaction occurs in the relatively confined regions under the overhanging gold film. Of more serious consequence is the edge definition of the silicon features generated in the RIE. Figure 5 shows the typical edge definition of the silicon structures in all areas exhibiting the granular perimeter band in the metal mask. Generally, it was observed that the width of this region tracked with the width of the pre-existing granular perimeter in the metal mask. The etch depth in these regions is reduced, as might be expected if a permeable barrier were offering only limited protection from the etchant gasses.

Figure 6 shows an electron micrograph of a typical submicron silicon feature produced in the RIE. It is currently unclear whether the narrow dimensions of the feature (about 300 nm) is a reflection of some isotropic character of the RIE or if the size is a consequence of the underlying nickel feature dimension in the metal mask. Electron microscopy of various samples has shown that nickel features in the metal masks have lateral dimensions typical of the silicon structure shown in figure 6. While obvious problems such as sidewall taper and surface roughening are present in this structure, the result is generally encouraging for future generation of submicron features using the microcontact printing technique. The

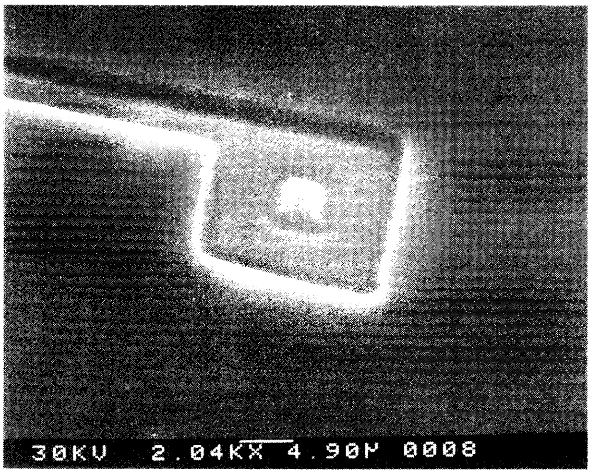

Figure 4. The patterned Si material, using CF_4/O_2 reactive-ion etching with the Au/Ni mask.

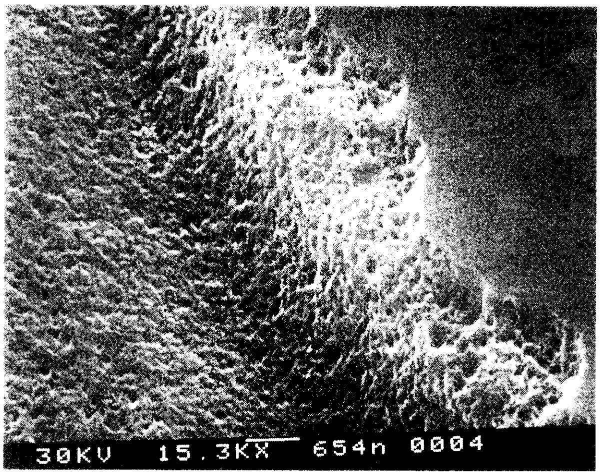

Figure 5. The edge definition of the etched Si. The roughness at the top is well correlated with the granularity of the over hanging gold layer. The micro-roughness of the walls and bottom surface is typical of RIE.

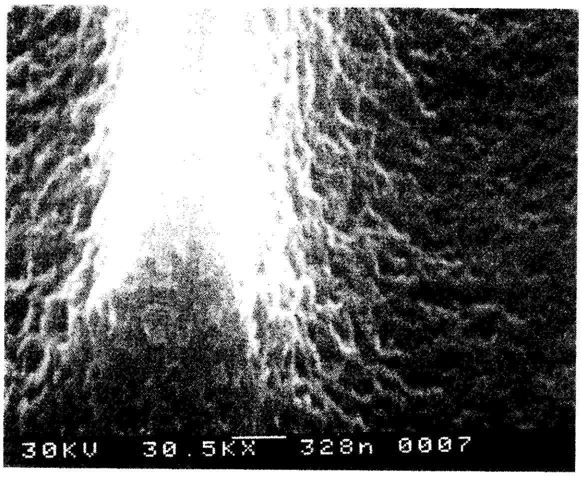

Figure 6. An etched line in the Si shows a typical resolution (width) of 0.3 μm.

fact that silicon feature dimensions of less than 500 nm can be generated using a hand held stamping technique suggests that the limit of more refined procedures using some variant of the methodology should be significantly lower.

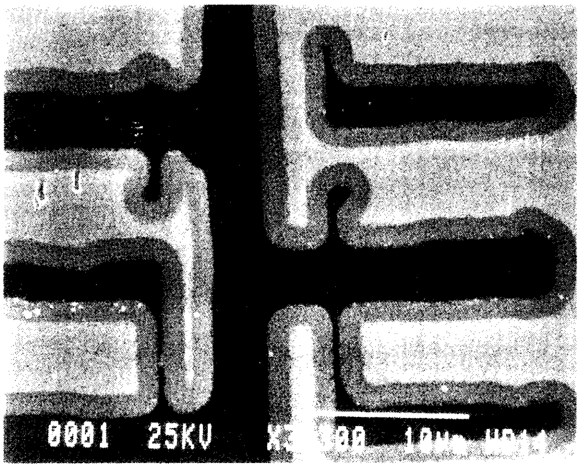

Figure 7. Test sample for nickel masked RIE (prior to Au removal) evaluation. The features marked with the arrows A are holes in the Au layer that will replicate through the process (subsequent figures). The narrow section (B) appears in the next figure.

As a test of whether the reduced dimensions observed in the underlying nickel layer could function as an effective mask in the RIE process and thus eliminate the problems associated with porous gold feature edges, a sample was selected for gold removal and RIE testing. Some mask damage was evident in the virgin sample, but it exhibited nickel feature dimensions appropriate for submicron feature production. The gold/nickel composite mask is shown in figure 7. Contrasting differences in the photo suggest that a nickel feature with appropriate dimensions existed and this feature was tracked throughout subsequent processing. Holes (A) in the overlying gold produce consequent structures in the final silicon itself. Figure 8 shows the nickel feature after SAM removal followed by gold etch using a cyanide solution. In this preliminary test, the SAM was removed with sulfuric acid and it is apparent that the nickel has been etched wherever the overlying gold was damaged. From figure 8, it may be seen that nickel features with lateral dimensions of about 300 nm were present on the silicon surface prior to RIE. The thin structure in the center of the figure is the feature labeled B in figure 7. Figures 9 and 10 show the resulting silicon structure after the sample had been processed in the RIE. All of the nickel structures, including those with dimensions in the submicron regime, have been reproduced in the silicon. The labeled features correlate to the equivalent labels in figure 7. The edge definition of the silicon structure is significantly improved over that observed when the gold overlayer was employed. A more controlled process, employing only nickel as the mask layer, may be preferable over the gold/nickel composite mask (figure 10).

4. Conclusion

Microcontact printing techniques employing self-assembled monolayers of alkanethiolate in the production of metal masks have been combined with reactive ion etch for subsequent pattern transfer to silicon. Silicon feature sizes of about 300 nm have been demonstrated. Some

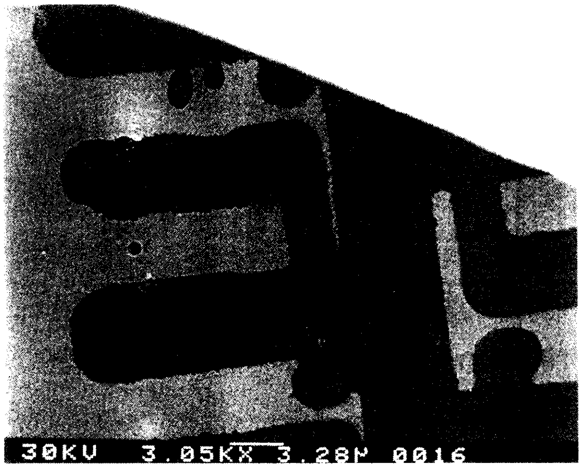

Figure 8. The Ni remaining after the removal of the Au in the cyanide etch. The narrow line in the center is feature B from figure 7.

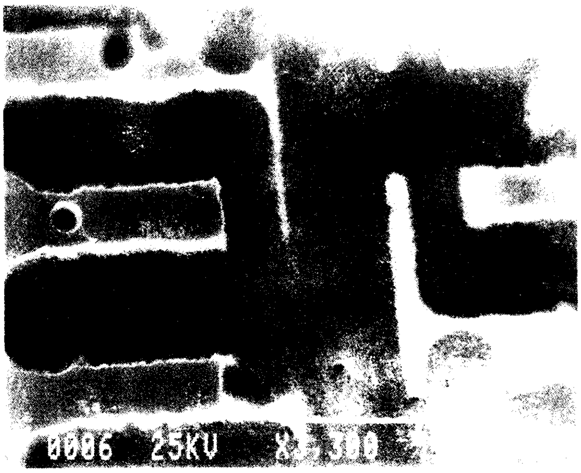

Figure 9. The Si after RIE processing using just the Ni mask. Features labeled A and B correlate to those so labeled in figure 7.

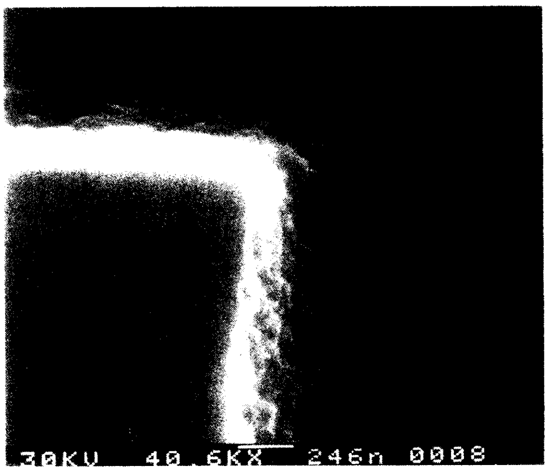

Figure 10. The Si after RIE using Ni masks. Edge resolution is much better than in RIE using Au/Ni masks.

inadequacies in the SAM-formed metal masks have been characterized by electron microscopy. Notably, the particular SAM used allowed penetration of the gold etchant through the SAM, compromising the pattern. Particularly, nickel etch control and metal feature edge definition also remain problems to be solved if the process is to be employed in submicron feature production. Nickel patterns produced in the process and used as masks without the gold overlayer were successful as masks in the RIE process and appear to give somewhat improved edge definition over processes in which the gold layer remains.

References

[1] Wolf S and Tauber R N 1986 *Silicon Processing for the VLSI Era* vol 1 (Sunset Beach, CA: Lattice)
[2] Calvert J M, Chen M-S, Dulcey C S, Georger J H, Peckerar M C, Schnur J M and Schoen P E 1991 *J. Vac. Sci. Technol.* B **9** 3447
[3] Calvert J M 1993 *J. Vac. Sci. Technol.* B **11** 2155
[4] Han J, Ferry D K and Newman P 1990 *IEEE Electron Dev. Lett.* **11** 209
[5] Randall J N, Reed M A, Moore T M, Matyi R J and Lee J W 1988 *J. Vac. Sci. Technol.* B **6** 302
[6] Yoshimura T, Nakayama Y and Okazaki S 1992 *J. Vac. Sci. Technol.* B **10** 2615
[7] Dulcey C S, Georger J H, Krauthamer V, Stenger D A, Fare T L and Calvert J M 1991 *Science* **252** 551
[8] Lercel M J, Tiberio R C, Chapman P F, Craighead H G, Sheen C W, Parikh A N and Allara D L 1993 *J. Vac. Sci. Technol.* B **11** 2823
[9] Bernstein G H, Liu W P, Khawaja Y N, Kozicki M N, Ferry D K and Blum L 1988 *J. Vac. Sci. Technol.* B **6** 2298
[10] Song H J, Rack M J, Abugharbieh K, Lee S Y, Khan V, Ferry D K and Allee D R *J. Vac. Sci. Technol.* **12** 3720
[11] Allgair J, Ryan J M, Song H J, Kozicki M N, Whidden T K and Ferry D K these proceedings
[12] Nuzzo R G and Allara D L 1983 *J. Am. Chem. Soc.* **105** 4481
[13] Chidsey C E D, Porter M D and Allara D L 1986 *J. Electrochem. Soc.* **133** 130
[14] Whitesides G M and Gorman C B *Handbook of Surface Imaging and Visualization* ed A T Hubbard (Boca Raton: CRC Press) in press
[15] Abbott N L, Folkers J P and Whitesides G M 1992 *Science* **257** 1380
[16] Tiberio R C, Craighead H G, Lercel M, Lau T, Sheen C W and Allara D L 1993 *Appl. Phys. Lett.* **62** 476
[17] Kuumar A, Biebuyck H A, Abbott N L and Whitesides G M 1992 *J. Am. Chem. Soc.* **114** 9188
[18] Lopez G P, Biebuyck H A, Frisbie C D and Whitesides G M 1993 *Science* **260** 647
[19] Calvert J M, Georger J H, Peckerar M C, Pehrsson P E, Schnur J M and Schoen P E 1992 *Thin Solid Films* **211** 359
[20] Lopez G P, Biebuyck H A, Harter R, Kumar A and Whitesides G M 1993 *J. Am. Chem. Soc.* **115** 10774
[21] Kumar A, Biebuyck H A and Whitesides G M 1994 *Langmuir* **10** 1498
[22] Wilbur J L, Kumar A, Kim E and Whitesides G M 1994 *Adv. Mater.* **7** 600
[23] Kim E, Kumar A and Whitesides G M 1995 *J. Electrochem. Soc.* **142** 678